https://doi.org/10.5194/amt-2020-34
Preprint. Discussion started: 18 February 2020

Atmospheric Measurement Techniques Discussions

Three-dimensional wind profiles using a stabilized shipborne cloud radar in wind profiler mode

Alain Protat[1], Ian McRobert[2]

[1] Australian Bureau of Meteorology, Melbourne, Victoria, Australia
[2] Engineering and Technology Program, CSIRO Oceans and Atmosphere, Hobart, Tasmania, Australia

Correspondence to: Alain Protat (alain.protat@bom.gov.au)

Abstract.

In this study, a shipborne 95 GHz Doppler cloud radar mounted on a stabilized platform is used to retrieve vertical profiles of three-dimensional (3D) winds by sequentially pointing the stabilized platform in different directions. A specific challenge is that the maximum angle off zenith is 8°, which implies that the projection of the horizontal wind components onto the radar beam directions is a small component of Doppler velocity in most cases. A variational 3D wind retrieval technique is then described, allowing for 1-minute resolution 3D wind profiles to be retrieved. Statistical comparisons with 3-hourly radiosonde launches and qualitative comparisons with ship-level horizontal winds demonstrate that accurate 3D wind profiles can be obtained from such cloud radar observations at small off-zenith angles.

1 Introduction

Vertically-pointing Doppler cloud radars, combined with cloud and aerosol backscatter lidars provide unique observations to better understand the interactions between dynamics and microphysics in clouds and light precipitation, aerosol – cloud interactions, and cloud radiative forcing. Doppler cloud radars are also extensively used to evaluate satellite products and the representation of cloud and precipitation properties in models. The focus of studies has been on retrieving the microphysical properties of clouds from either the cloud radar alone (e.g., Matrosov et al. 2002; Mace et al. 2002; Delanoë et al. 2007), the lidar alone (e.g., Heymsfield et al. 2005), or the combination of the two (Wang and Sassen 2002; Okamoto et al. 2003; Tinel et al. 2005; Delanoë and Hogan 2008, Deng et al. 2010). In contrast, not much has been done to characterize the dynamical context of these cloud microphysical observations, including horizontal winds and vertical wind shear which are needed to better understand the internal cloud dynamics and entrainment processes within and at the boundaries of clouds.

Scanning cloud radars were recently developed to describe clouds in three dimensions (3D) from ground-based observatories. However, very little has been done so far to characterize the 3D wind profiles at high vertical resolution within clouds using such measurements, as typical scanning strategies focus on describing the morphological structure using Plane Position Indicator (PPI, scanning in azimuth at successive constant elevations) or Range Height Indicator (RHI, scanning different elevations at constant azimuth) scanning sequences. UHF and VHF profilers provide such 3D wind profiles in clear-air and precipitation using the so-called "profiler mode", which consists in alternating vertical pointing with off-zenith pointing by about 15-20° in two perpendicular directions (North and East for instance). The only issue with UHF and VHF wind profilers is that they lack the sensitivity to detect thin non-precipitating clouds.

In this study, we report on a pilot study using a shipborne cloud radar on a stabilized platform to derive high-resolution vertical profiles of 3D wind. The idea is to use the stabilized platform to point in a series of different directions. However, when the cloud radar is used on the Marine National Facility (MNF) Research Vessel (RV) *Investigator*, the maximum angle off zenith that can be safely used is ±8° in pitch and roll directions. This is lower than typical angles of ±15-20° used for wind profilers. The main objective of this pilot study is to assess whether high-quality 3D winds can be retrieved from such small angles off zenith. As this study was conducted during a major field experiment, the Years of the Maritime Continent – Australia (YMCA), radiosondes were launched every three hours, allowing for some quantitative comparisons with the retrieved cloud radar 3D wind profiles. In section 2, we briefly describe the cloud radar, the stabilized platform and implemented scanning sequences. In section 3, we analyse case studies and evaluate the cloud radar 3D winds against radiosonde measurements. Conclusions are finally given in section 4.

2 Description of the pilot study

As described in section 1, the main objective of this pilot study is to assess whether vertical profiles of 3D winds can be derived from pointing the stabilized platforms in a series of different angles ±8° off zenith. In this section we briefly describe the cloud radar, the stabilized platform and implemented sampling strategies, and the 3D wind retrieval technique.

2.1 The BASTA Doppler cloud radar

The research-grade BASTA Doppler cloud radar is described in detail in Delanoë et al. (2016). It is a frequency-modulated continuous wave (FMCW) radar operating at a frequency of 95 GHz. The radar uses two Cassegrain dishes (60 cm in diameter) and all the electronic components are installed in a pressurized and insulated box. The data acquisition and processing are done using a field-programmable gate array (FPGA). This cloud radar uses a low-power solid-state transmitter (0.5W) and estimates both reflectivity and Doppler velocity using the pulse-pair processing technique with 2048 samples, allowing for high Doppler measurement accuracy. During the YMCA field experiment, a 12 seconds sequence split into four successive modes (each mode with an acquisition and processing time of 3 seconds) was designed and used to capture both low-level clouds and light precipitation with high vertical resolution and tropical cirrus clouds with high sensitivity. The respective vertical resolutions of these four modes are 12.5m, 25m, 100m (moderate sensitivity), and 100m (higher sensitivity but shorter Nyquist velocity). The approximate minimum detectable signal of these four modes is -28, -34, -40, and -43 dBZ @ 1 km range, respectively. This sensitivity is lower than that reported in Delanoë et al. (2016), due to current issues with the antenna alignment. This lower sensitivity is not detrimental to our pilot study.

2.2 The *RV Investigator* stabilized platform and sampling strategies

When used on *RV Investigator*, the BASTA cloud radar is mounted on a stabilized platform inside an air-conditioned container, making operations in harsh environments such as the Southern Ocean, Antarctica and the Tropics a smooth experience. The stabilized platform design is described in detail in Filisetti et al. (2017) and follows the design from Moran et al. (2012). It has been recently demonstrated that vertical stabilization to better than 0.2° can be achieved with this platform for sea states up to 6. In this shipborne configuration, the plexiglass dome of the BASTA cloud radar is removed and replaced by a bigger one mounted directly on the container roof. Due to the size of the open cut on the container roof and the requirement to minimize contaminations of the signal by multiple reflections on the metallic structure inside the container, the top of the cloud radar is lifted very close to the dome. This configuration limits the possible rotation in pitch and roll directions to about 12° from the vertical of the container. Our experience from the Southern Ocean high seas is that with the anti-roll system of *RV Investigator* this value of 12° has been exceeded less than 1% of the time.

The baseline operating mode in earlier deployments was the "vertical mode", where the instrument is stabilized to point vertically all the time. For this pilot study we have developed an additional mode, referred to as the "profiler mode" in the following, which consists of a 120 seconds sequence with 15 seconds spent at the following 8 pointing angles: vertical, +8° pitch, vertical, +8° roll, vertical, -8° pitch, vertical, -8° roll. With such a sequence, we still retain a high temporal resolution for the vertical observations while being able to retrieve 3D wind profiles at 1-minute resolution from any of four successive pointing angles. The rationale for using positive and negative pointing angles is to assess whether the same 3D wind profiles can be derived from these different combinations of angles. Note that the time (about 1.5s) required to move from one angle to the next is included in the 15 seconds. The selected time resolution of 15 seconds is a trade off to make sure that we are collecting data from all four radar modes (which takes 12 seconds) for each pointing direction while still retaining a high temporal resolution (1 minute) for the retrieved 3D wind profiles. The 8° angle selected for this mode is also a trade-off between allowing enough projection of the horizontal wind components onto the radar beams off zenith and the need to stabilize the instrument in that direction accurately. Using 8° means that we can only stabilize the instrument for motions less than about 4°. Although this will present a challenge in rough seas such as over the Southern Ocean, such motion was never encountered during the YMCA experiment.

2.3 The 3D wind retrieval technique

When operating in vertical mode, Doppler velocities are simply corrected for heave rates (the vertical component of ship speed) using the 10 Hz ship positioning system data (same as in Moran et al. 2012). When operating in modes with off zenith pointing, Doppler velocities need to be corrected for both heave rates and ship horizontal speed. During the YMCA, we mostly stayed on station and heave was very low. As a result, Doppler corrections very rarely exceeded absolute values of 0.2 ms^{-1}. However, it will not be the case for future deployments. Therefore, below we develop the full set of equations for the 3D wind retrieval including all corrections.

A variational 3D wind retrieval has been adapted for the profiler mode sampling strategy from the dual-Doppler weather radar technique of Protat and Zawadzki (1999). The three "control variables", i.e., the quantities to be retrieved, are the zonal (eastward) horizontal wind component V_X *(nt, nz)*, the meridional (northward) horizontal wind component V_Y *(nt, nz)* and V_Z *(nt, nz)* = *W (nt, nz)* + V_T *(nt, nz)*, where *W (nt, nz)* is the vertical wind component and V_T *(nt, nz)* is the terminal fall velocity of hydrometeors, *nt* is the number of time steps per retrieval day and *nz* is the number of vertical levels for the vertical profiles. The *nt* and *nz* parameters can be adjusted for different applications. When operating in profiler mode instead of the traditional weather radar PPI sampling which mostly involves low elevation angles above the horizontal plane, the anelastic airmass continuity equation and the constraint that the vertical air velocity at ground is nil are not needed as part of the retrieval process. As a result, only the Doppler velocity constraint from the Protat and Zawadzki (1999) formalism is used and includes all pointing angles to retrieve the vertical profiles of 3D wind. As a result, the cost function to be minimized can be simply written as:

$$J = \sum_{i=0}^{nt} \sum_{k=0}^{nz} \left(V_R\,(i,k) - V_R'\,(i,k) \right)^2 \qquad (1)$$

Where

$$V_R'\,(i,k) = \left(V_X\,(i,k) - U_{ship}(i)\right) cos\,\left(az(i)\right) cos\,\left(el(i)\right) + \left(V_Y\,(i,k) - V_{ship}(i)\right) sin\,\left(az(i)\right) cos\,\left(el(i)\right) + \left(W\,(i,k) + V_T\,(i,k) - W_{ship}(i)\right) sin\,\left(el(i)\right) \qquad (2)$$

With $V_R\,(i,k)$ the measured Doppler velocities, $V_R'\,(i,k)$ the theoretical Doppler velocities which need to match the observed Doppler velocities $V_R\,(i,k)$ at the end of the minimization process, $(U_{ship}(i), V_{ship}(i), W_{ship}(i))$ the three components of the ship speed producing apparent Doppler velocity in the cloud radar measurements which need to be subtracted to the theoretical Doppler velocities, and $(az(i), el(i))$ the azimuth angle of each radar beam with respect to the east (positive counter-clockwise) and the elevation angle of each radar beam with respect to the horizontal (positive upwards).

The different steps of the procedure to minimize the cost function *J* can be summarized as follows: 1) make an initial guess of the control variables (V_X, V_Y, V_Z) – we use zero by default ; 2) calculate the gradient of the cost function with respect to the control variables (as explained in Protat and Zawadzki 1999); 3) exit if the predefined convergence criterion is met; otherwise, 4) calculate a new guess of (V_X, V_Y, V_Z) using the conjugate–gradient method (Powell 1977); and 5) return to step 2 for a new iteration using this new guess until the convergence criterion is met. Once V_Z is obtained, previous studies have shown that its two components, *W* and V_T, can be separated using statistical approaches relating reflectivity to V_T (see description of different possible techniques and expected performance in Protat and Williams, 2011). However, since there is no reference observation to evaluate this in our dataset, this separation of *W* and V_T has not been included in the present analysis.

https://doi.org/10.5194/amt-2020-34
Preprint. Discussion started: 18 February 2020

Atmospheric Measurement Techniques Discussions

3 Results

The pilot study to test the new wind profiler mode was conducted during the YMCA field experiment (12 November 2019 – 17 December 2019). Large-scale conditions during the experiment were very unfavourable for the development of major mesoscale convective systems and associated cloud anvils and tropical cirrus layers. Nevertheless, a variety of cloud cover types has been sampled over that period. In this section, we present results obtained for four very different cases to illustrate the capability to retrieve 3D winds from the cloud radar in profiler mode in different situations. The first case is a stratiform precipitation case which developed on 23-24/11/2019 within a horizontal flow characterized by multiple vertical wind shear layers. This case was over the ship for about seven hours. The second case is a shallow cumulus congestus case which developed in the evening of 24/11/2019 in a high low-level vertical wind shear environment, as measured by the soundings. The third and fourth cases are an altostratus and a tropical cirrus outflow, which both detrained from surrounding deep convective activity on 04/12/2019.

Two types of measurements are used in this study to evaluate the retrieved horizontal winds, both bringing complementary insights. Note that we do not have independent measurements to assess the vertical wind component. However, this component is directly measured with the current sampling strategy so can be assumed accurate to within measurement and Doppler corrections uncertainties. The first measurements are ship-level horizontal winds measured at 24m height on the front mast by two automatic weather stations. Comparisons are made with the first valid radar range bin where winds can be retrieved (usually about 100m height). The limitations of such comparisons are the difference in heights of the measurements, and the fact that it does not allow for an assessment of the full vertical profiles, only those situations when low clouds are present. The second type of measurements is soundings (Vaisala RS41-SGP radiosondes), which were launched every three hours during YMCA. This second source of validation has the major advantage of providing full vertical profiles of horizontal winds surrounding the cloud radar retrievals. However, balloons take about one hour to reach the tropopause in the Tropics and can drift by tens of kilometres from the initial launch location over that period. As a result, these measurements can only really be used for point-by-point, quantitative comparisons with the 3D wind retrievals in the low levels in all wind conditions up to mid-levels in light wind conditions. However, measurements from soundings do provide qualitative information on the upper-level winds surrounding the retrieved 3D wind profiles.

These advantages and limitations have informed the way comparisons are made in this section. Low-level time series of horizontal wind components have been averaged using the two wind estimates from the weather stations and are displayed on the vertical cross-sections of retrieved winds at altitude zero with the same colour code. For radiosonde comparisons, we have selected individual periods of interest, from which we have produced joint horizontal wind – height distributions for each period to quantify the 3D wind retrieval variability between soundings and superimposed the horizontal wind profiles measured by the soundings within each of these periods. All these comparisons are essentially of a qualitative nature but allow for a good visual assessment of the retrieved 3D wind profiles. Again, lower-level comparisons with the soundings provide a much more quantitative assessment than upper-level ones, owing to a much better spatial match between cloud radar and sounding measurements.

Figs. 1-3 show results obtained for the stratiform precipitation case. The sum of vertical air motion and terminal fall speed of hydrometeors (top panel of Fig. 1) is characterized by an expected sharp transition from downward vertical motions in the -2 to 0 ms^{-1} range in ice phase above the melting layer height (around 4.5 km), to values below -4 ms^{-1} in liquid phase, below the melting layer height. Stratiform regions are generally characterized by relatively small vertical air motions, rarely exceeding 0.5 ms^{-1} (e.g. Protat and Williams, 2011, in the same Darwin region). As a result, the sum is generally dominated by terminal fall speed. Layers of enhanced downward motions in ice phase closer to the melting layer result from the aggregation of ice crystals producing bigger particles as they fall within the stratiform region, as documented in several studies. Values of near zero vertical motions are also found near cloud top, which is also the expected signature of much smaller ice crystals falling at a much lower speed. The two retrieved horizontal wind components (middle and bottom panels of Fig. 1) are characterized by long-lasting structures of higher easterly and south-westerly winds just below (2 – 4 km height) and just above (6 – 8 km height) the melting layer, respectively. An upper-level south-westerly jet is also clearly visible on the retrieval (above 10 km height). Qualitative validation of the low-level winds is shown in Fig. 2. Except for a short period after midnight where some clear differences are observed, the agreement between ship horizontal winds and retrieved winds is good, with subtle changes in wind speed and direction picked up in the retrieval. Looking more closely at the ship time series, it appears that this short period is characterized by very large differences in excess of 10 ms^{-1} between the port and starboard weather station estimates, with our retrieved values being closer to one of the estimates. A more quantitative and statistical comparison of the retrieved vertical profiles of the horizontal wind components with the radiosonde observations is shown in Fig. 3 (radiosondes are also superimposed to retrievals in Fig. 1) for the two 4-hours periods depicted in Fig.1. For each period we have two radiosonde profiles to compare with. Comparing profiles from the two radiosondes indicates that there is substantial variability of the zonal wind component above 6 km height for the first period (top panels of Fig. 3). The retrieved horizontal winds closely match the radiosonde profiles below 5 km height, and the agreement is also very good in the upper levels, with the two radiosonde observations generally bounding the retrieved horizontal wind distributions. Given the spatial and temporal mismatch between these two sources of data, we conclude that these comparisons clearly demonstrate that accurate vertical profiles of horizontal wind can be derived from the cloud radar using the proposed profiler mode, despite the small 8° off zenith angles used. The purpose of the remaining figures of this study is to demonstrate that this good agreement for the stratiform precipitation case holds true for different types of cloud cover, including a cumulus congestus case characterized by high vertical wind shear (Figs. 4 and 5), an altostratus case in a very light wind environment (Figs. 6 and 7), and a tropical cirrus case embedded in a north-westerly jet (Figs. 6 and 7).

4 Conclusions

In this study, we have used dedicated shipborne Doppler cloud radar observations around Darwin, Australia, to evaluate the potential of retrieving vertical profiles of 3D winds using a stabilized platform pointing in successive off-zenith directions at regular intervals. A challenge with using such setup is that the maximum off-zenith angle is 8°, which does not correspond to a large projection of the horizontal wind components onto the radar beam directions. Using this 8° value currently implies that only ship motions up to 4° in any direction can be compensated for by the stabilized platform. Taking advantage of this "profiler mode" sampling, we have developed a variational 3D wind retrieval technique allowing for 1-minute resolution 3D wind profiles to be estimated. Fully quantitative validation of the results was challenging, as there are no directly collocated observations in time or space available. However, statistical comparisons with radiosonde launches every 3 hours, and qualitative comparisons with ship-level horizontal winds demonstrated that accurate 3D wind profiles could be derived from such cloud radar observations at small off-zenith angles for a large variety of cloud cover types encountered during the field experiment. Given the positive results obtained with 8° angles, we will test even lower angles during our next shipborne field experiment. If satisfying results are obtained at even lower angles, this would improve our capability to retrieve 3D winds in much rougher seas than those encountered during the YMCA experiment.

Acknowledgments

The Authors wish to thank the CSIRO Marine National Facility (MNF) for its support in the form of *RV Investigator* sea time allocation on Research Voyage IN2019_V06, support personnel, scientific equipment, and data management. All Doppler cloud radar, radiosonde, and ship underway data are currently available upon request to Alain Protat (alain.protat@bom.gov.au) and will be publicly available by June 2020 in accordance with MNF policy from the CSIRO Data Access Portal (https://data.csiro.au/dap/).

Code availability

Code is not available publicly but can be shared upon request to Alain Protat (alain.protat@bom.gov.au).

Data availability

All data used in this paper are currently available upon request to Alain Protat (alain.protat@bom.gov.au) and will be publicly available by September 2020 in accordance with the Australian Marine National Facility policy from the CSIRO Data Access Portal (https://data.csiro.au/dap/).

Sample availability

No samples were used in this study.

Author contribution

AP and IM collected the datasets used in this study. IM designed the stabilized platform operating modes. AP analysed the cloud radar and radiosonde observations and wrote the manuscript.

Competing interests:

The authors declare that they have no conflict of interest.

References

Delanoë, J., A. Protat, J.-P. Vinson, W. Brett, C. Caudoux, F. Bertrand, J. Parent du Chatelet, R. Hallali, L. Barthes, M. Haeffelin, and J.-C. Dupont: BASTA, a 95 GHz FMCW Doppler radar for cloud and fog studies, J. Atmos. Oceanic Tech., 33, 1023-1038, 2016.

Delanoë, J., and R. J. Hogan: A variational scheme for retrieving ice cloud properties from combined radar, lidar, and infrared radiometer, J. Geophys. Res., 113, D07204, doi:10.1029/2007JD009000, 2008.

Delanoë, J., A. Protat, D. Bouniol, A. J. Heymsfield, A. Bansemer, and P. R. Brown: The characterization of ice cloud properties from Doppler radar measurements, J. Appl. Meteor., 46, 1682–1698, 2007.

Deng, M., G. G. Mace, Z. Wang, and H. Okamoto: Tropical Composition, Cloud and Climate Coupling Experiment validation for cirrus cloud profiling retrieval using CloudSat radar and CALIPSO lidar, J. Geophys. Res., 115, D00J15, doi:10.1029/2009JD013104, 2010.

Filisetti, A., A. Marouchos, I. McRobert, B. Baldwinson, A. Protat, and B. Atkinson: Design of an instrument stabilising system for in-situ measurements on a research vessel. In: Oceans '17 MTS/IEEE Aberdeen; 19/6/17 - 22/6/17; Aberdeen, Scotland. Aberdeen, UK: IEEE Xplore. 7. https://doi.org/10.1109/OCEANSE.2017.8084695, 2017.

Heymsfield, A. J., D. Winker, and G.-J. van Zadelhoff: Extinction-ice water content-effective radius algorithms for CALIPSO, Geophys. Res. Lett., 32, L10807, doi:10.1029/2005GL022742, 2005.

Mace, G. G., A. J. Heymsfield, and M. R. Poellot: On retrieving the microphysical properties of cirrus clouds using the moments of the millimeter-wavelength Doppler spectrum, J. Geophys. Res., 107.4815, doi:10.1029/2001JD001308, 2002.

Matrosov, S. Y., A. V. Korolev, and A. J. Heymsfield: Profiling Cloud Ice Mass and Particle Characteristic Size from Doppler Radar Measurements, *J. Atmos. Oceanic Technol.*, *19*, 1003–1018, 2002.

Moran, K., S. Pezoa, C. Fairall, C. Williams, T. Ayers, A. Brewer, S. P. de Szoeke and V. Ghate: A Motion-Stabilized W-Band Radar for Shipboard Observations of Marine Boundary-Layer Clouds, Boundary-Layer Meteorology, 143, 3-24, 2012.

Okamoto, H., S. Iwasaki, M. Yasui, H. Horie, H. Kuroiwa, and H. Kumagai: An algorithm for retrieval of cloud microphysics using 95-GHz cloud radar and lidar, J. Geophys. Res., 108, 4226, doi:10.1029/2001JD001225, 2003.

Powell, M. J.: Restart procedures for the conjugate-gradient method. Math. Prog., 11, 42–49, 1977.

Protat, A., and C. Williams: The accuracy of radar estimates of terminal fall speed from vertically-pointing Doppler cloud radar measurements, J. Appl. Meteor. Clim, 50, 2120-2138, 2011.

Protat, A., and I. Zawadzki: A variational method for real-time retrieval of three-dimensional wind field from multiple-doppler bistatic radar network data, J. Atmos. Oceanic Technol., 16 (4), 432-449, 1999.

Tinel, C., J. Testud, J. Pelon, R. Hogan, A. Protat, J. Delanoë, and D. Bouniol: The retrieval of ice cloud properties from cloud radar and lidar synergy, J. Appl. Meteor., 44, 860-875, 2005.

Wang, Z., and K. Sassen: Cirrus Cloud Microphysical Property Retrieval Using Lidar and Radar Measurements. Part I: Algorithm Description and Comparison with In Situ Data, J. Appl. Meteor., 41, 218–229, 2002.

https://doi.org/10.5194/amt-2020-34
Preprint. Discussion started: 18 February 2020

Atmospheric Measurement Techniques
Discussions

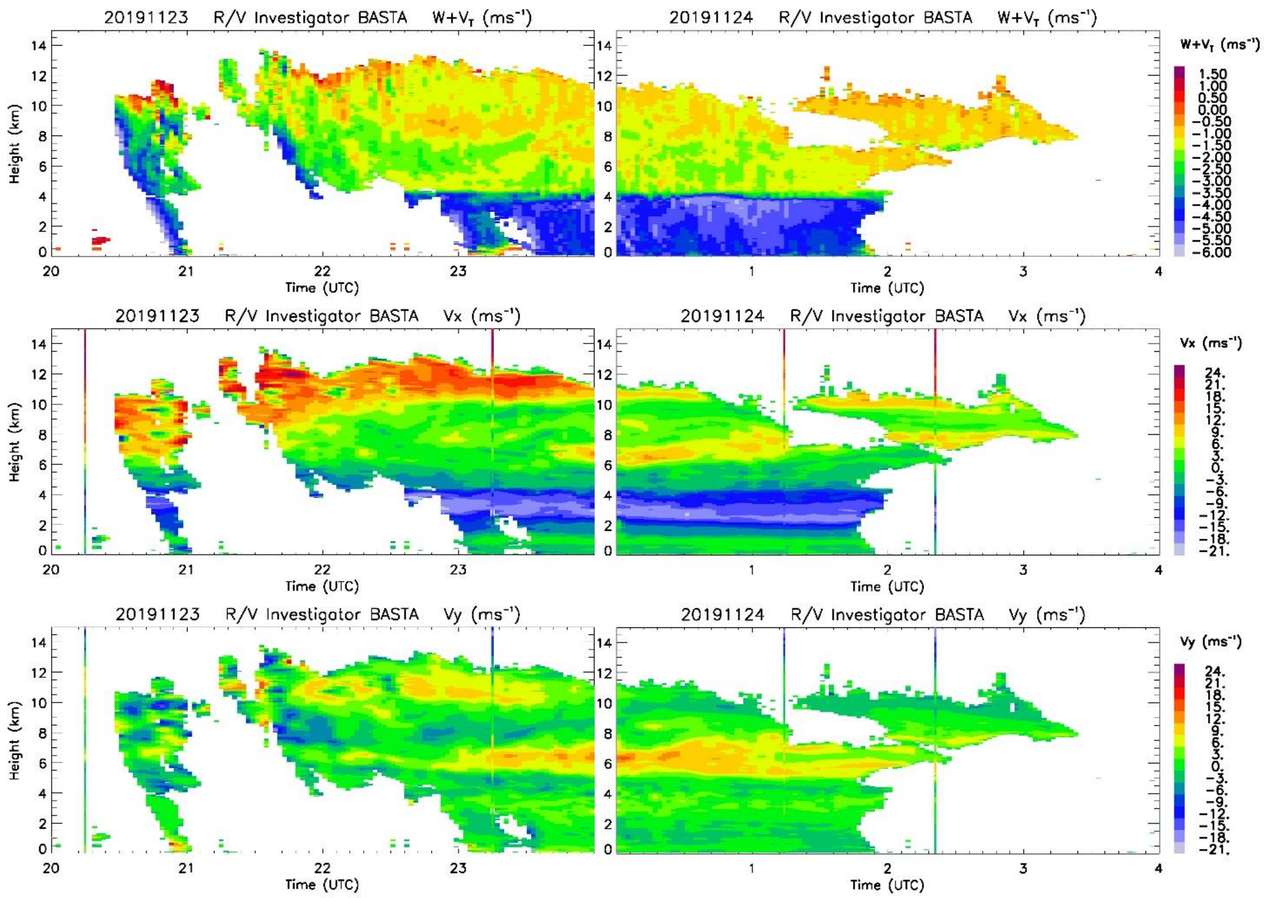

Figure 1: Time – height cross section of retrieved *W+V*$W+V_T$ (up), V_X (middle), and V_Y (bottom) in a stratiform precipitation case sampled on 23-24/11/2019 by the BASTA cloud radar on *RV Investigator*. Vertical lines on the middle and bottom panels are the horizontal wind components measured by the soundings. The reference time for the soundings is the launch time at ground.

https://doi.org/10.5194/amt-2020-34
Preprint. Discussion started: 18 February 2020

Atmospheric Measurement Techniques
Discussions

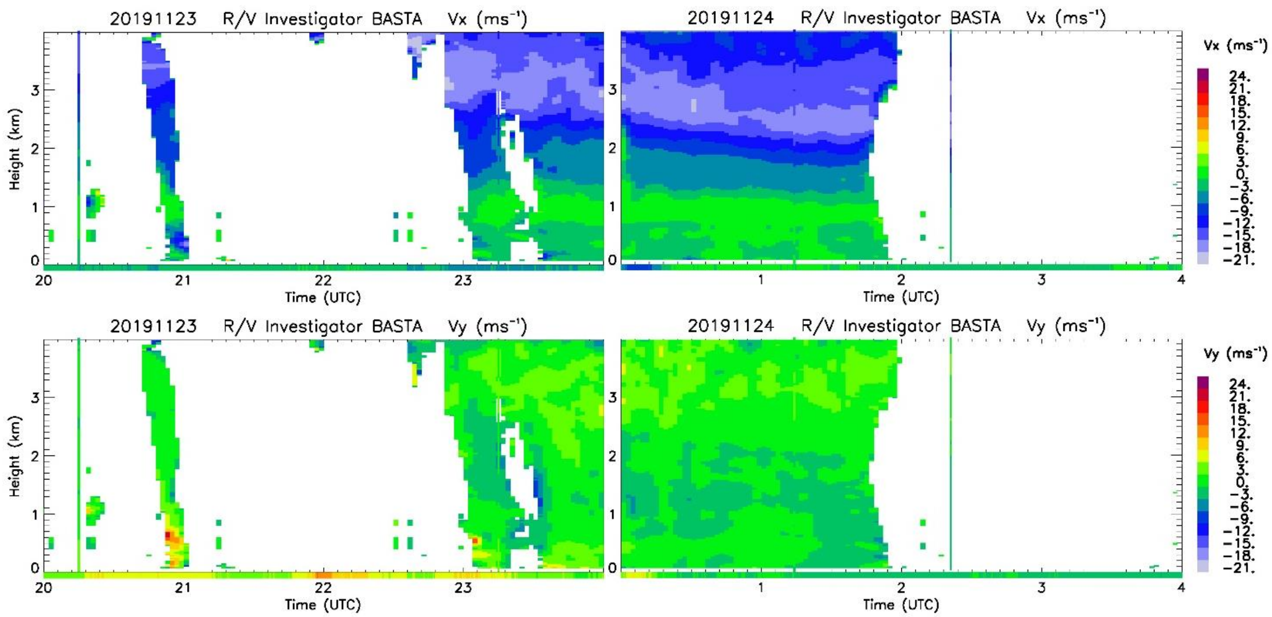

Figure 2: Time – height cross section of retrieved V_X (top) and V_Y (bottom) in the same case as Fig. 1 but for a maximum altitude of 4 km. The horizontal winds measured on the front mast of *RV Investigator* are displayed at height = 0 with the same colour scale as the retrieved winds.

https://doi.org/10.5194/amt-2020-34
Preprint. Discussion started: 18 February 2020

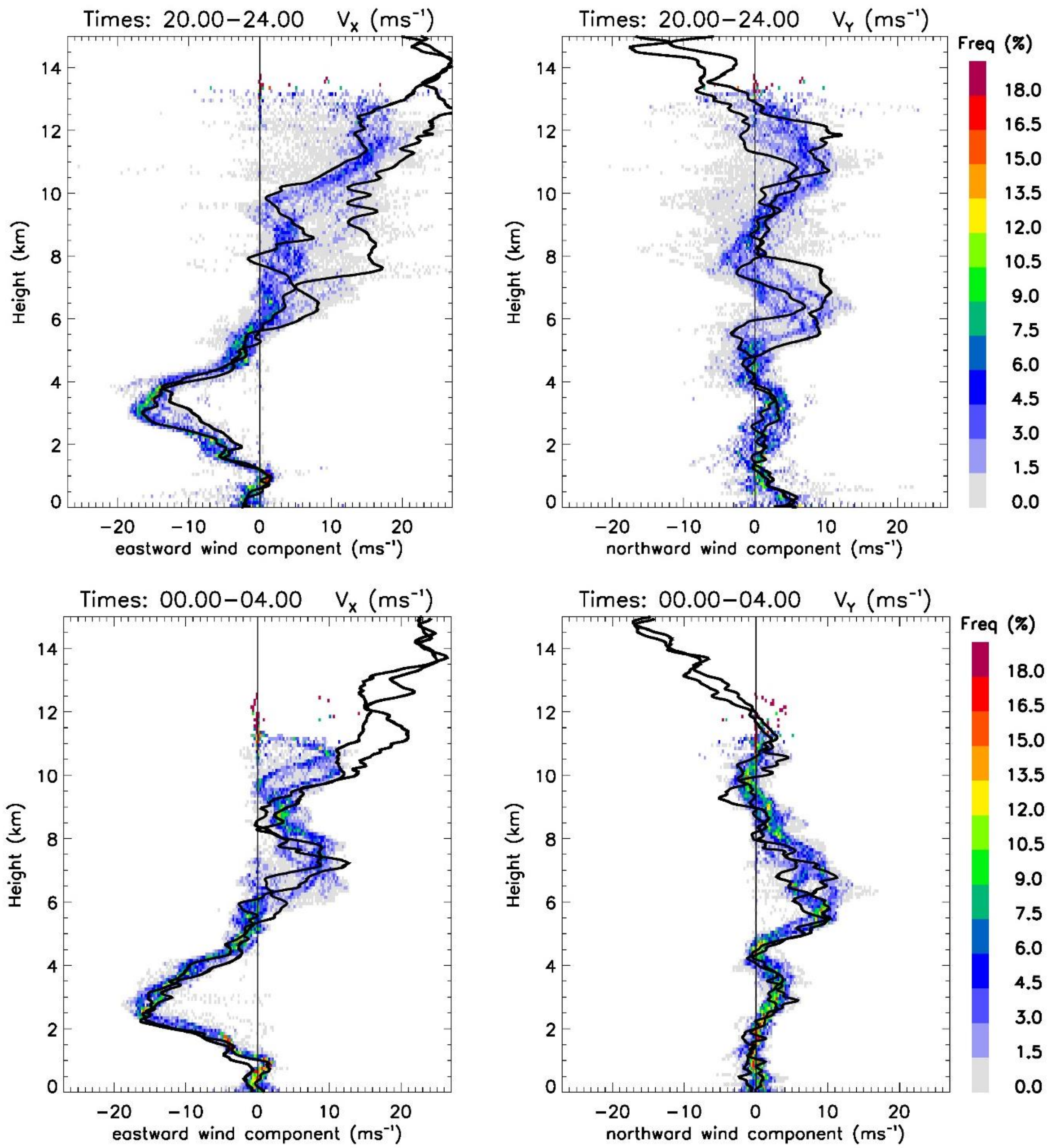

Figure 3: Comparison of V_X (left) and V_Y (right) joint wind – height frequency distributions (colours) and the same horizontal wind components measured by soundings for two time periods: 2000-2400 UTC on 23/11/2019 with sounding launches at 2015 and 2315 UTC (top panels) and 0000-0400 UTC on 24/11/2019 with sounding launches at 0115 and 0245 UTC (bottom panels).

https://doi.org/10.5194/amt-2020-34
Preprint. Discussion started: 18 February 2020

Atmospheric Measurement Techniques Discussions

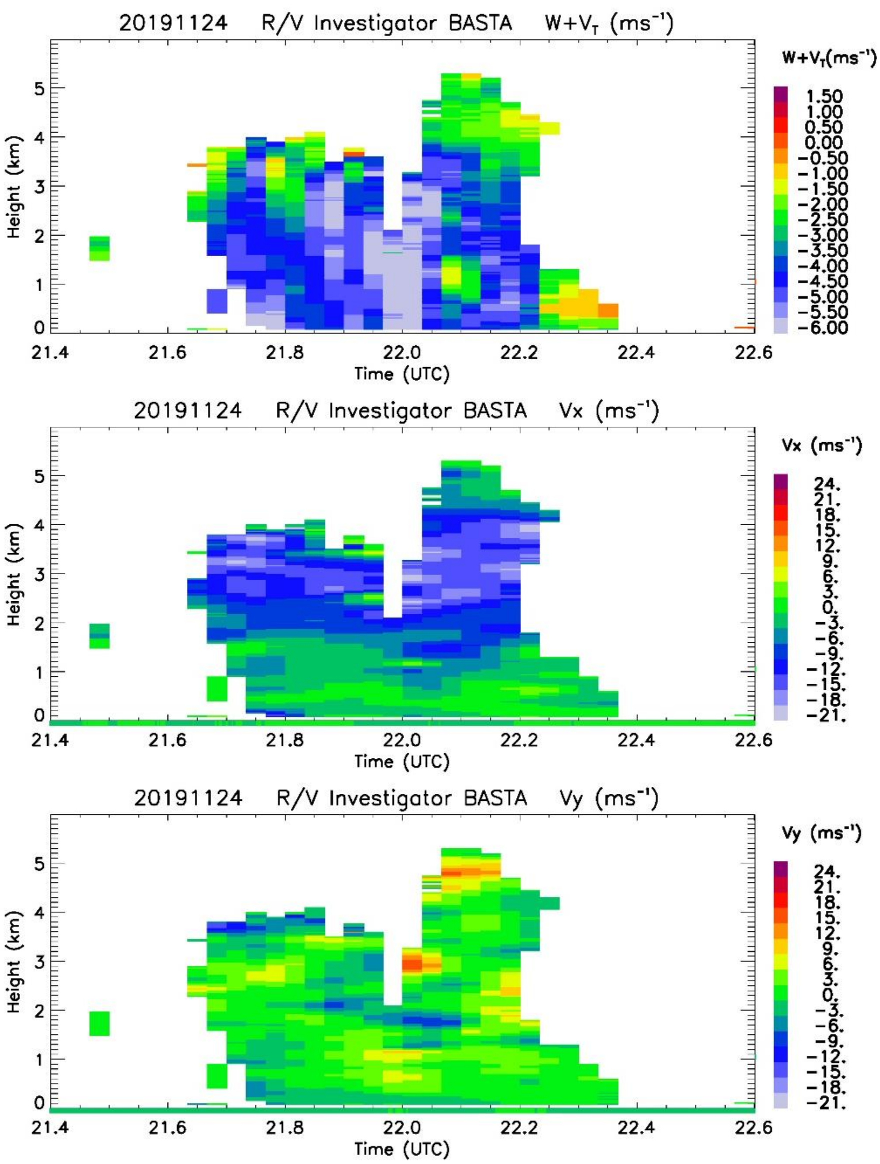

Figure 4: Same as Fig.2 but for the cumulus congestus case on 24/11/2019 and a maximum display height of 6 km.

290

https://doi.org/10.5194/amt-2020-34
Preprint. Discussion started: 18 February 2020

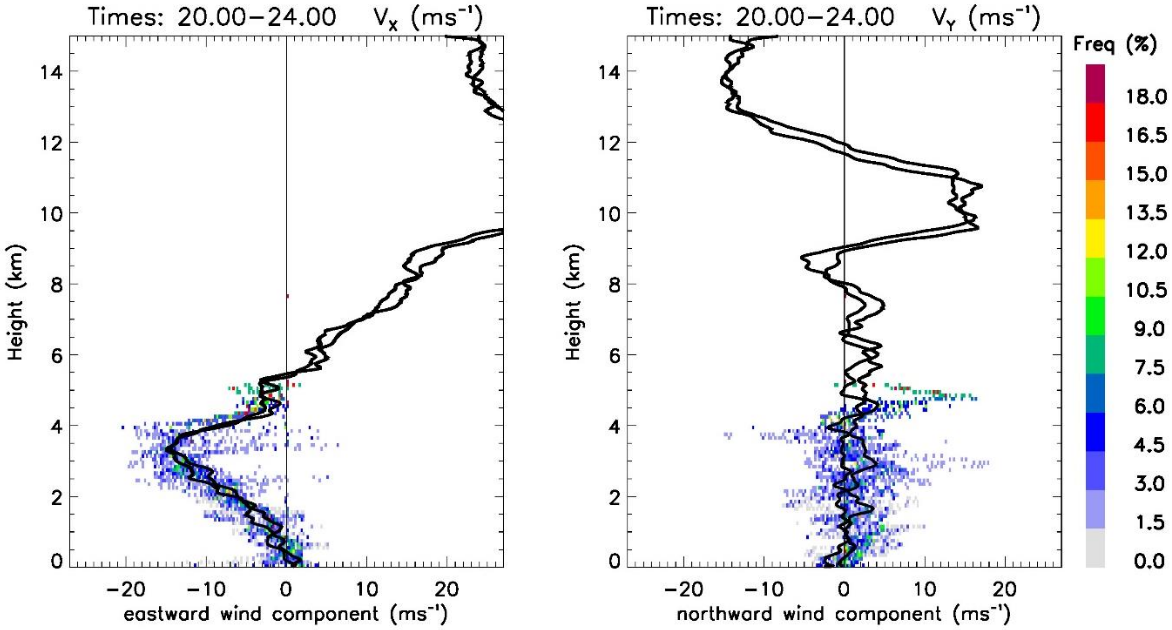

Figure 5: Same as Fig.3 but for the cumulus congestus case and the 2000-2400 LT period on 24/11/2019.

https://doi.org/10.5194/amt-2020-34
Preprint. Discussion started: 18 February 2020

Atmospheric Measurement Techniques
Discussions

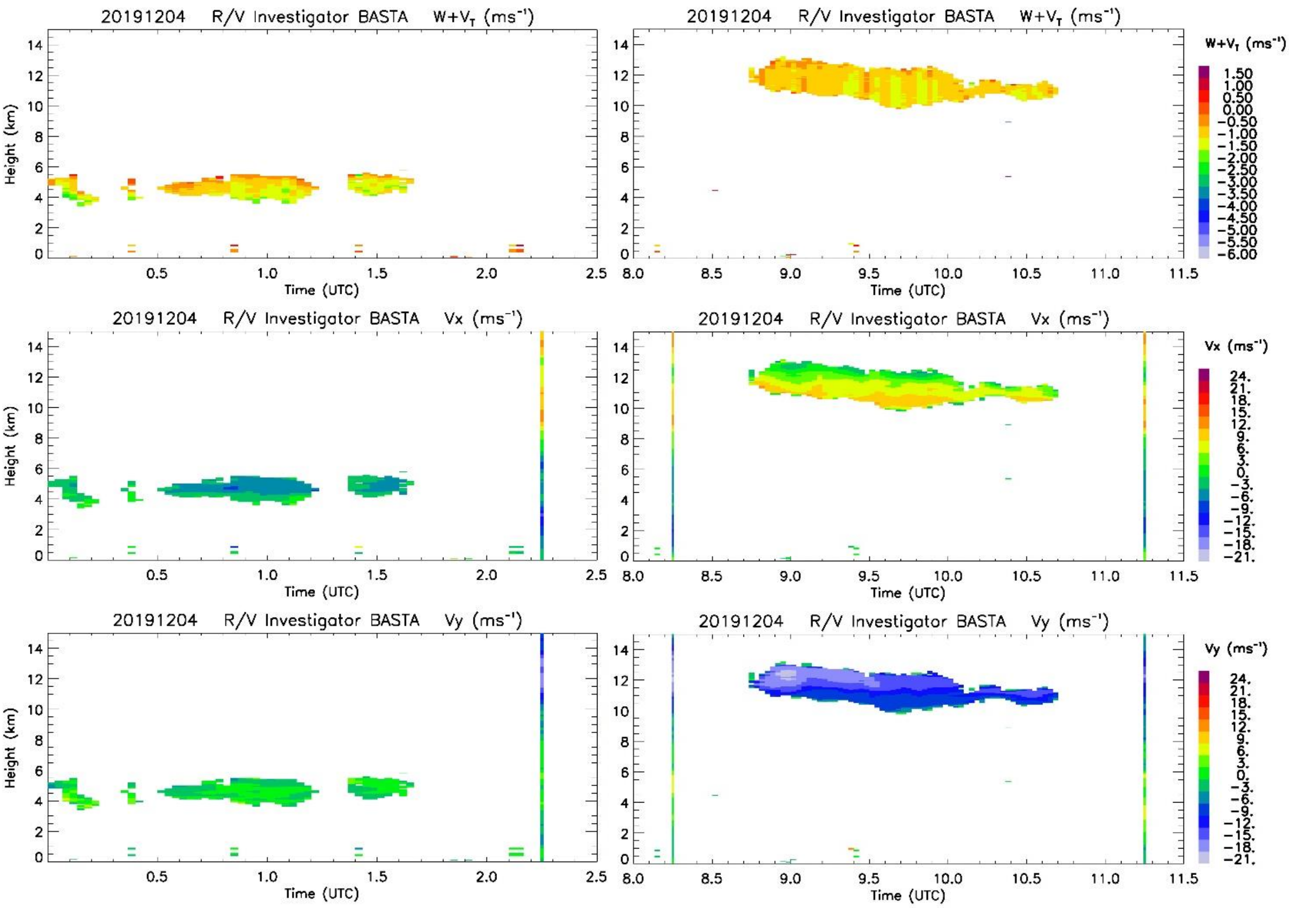

Figure 6: Same as Fig. 1 but for the altostratus (left) and tropical cirrus (right) cases sampled on 04/12/2019

https://doi.org/10.5194/amt-2020-34
Preprint. Discussion started: 18 February 2020

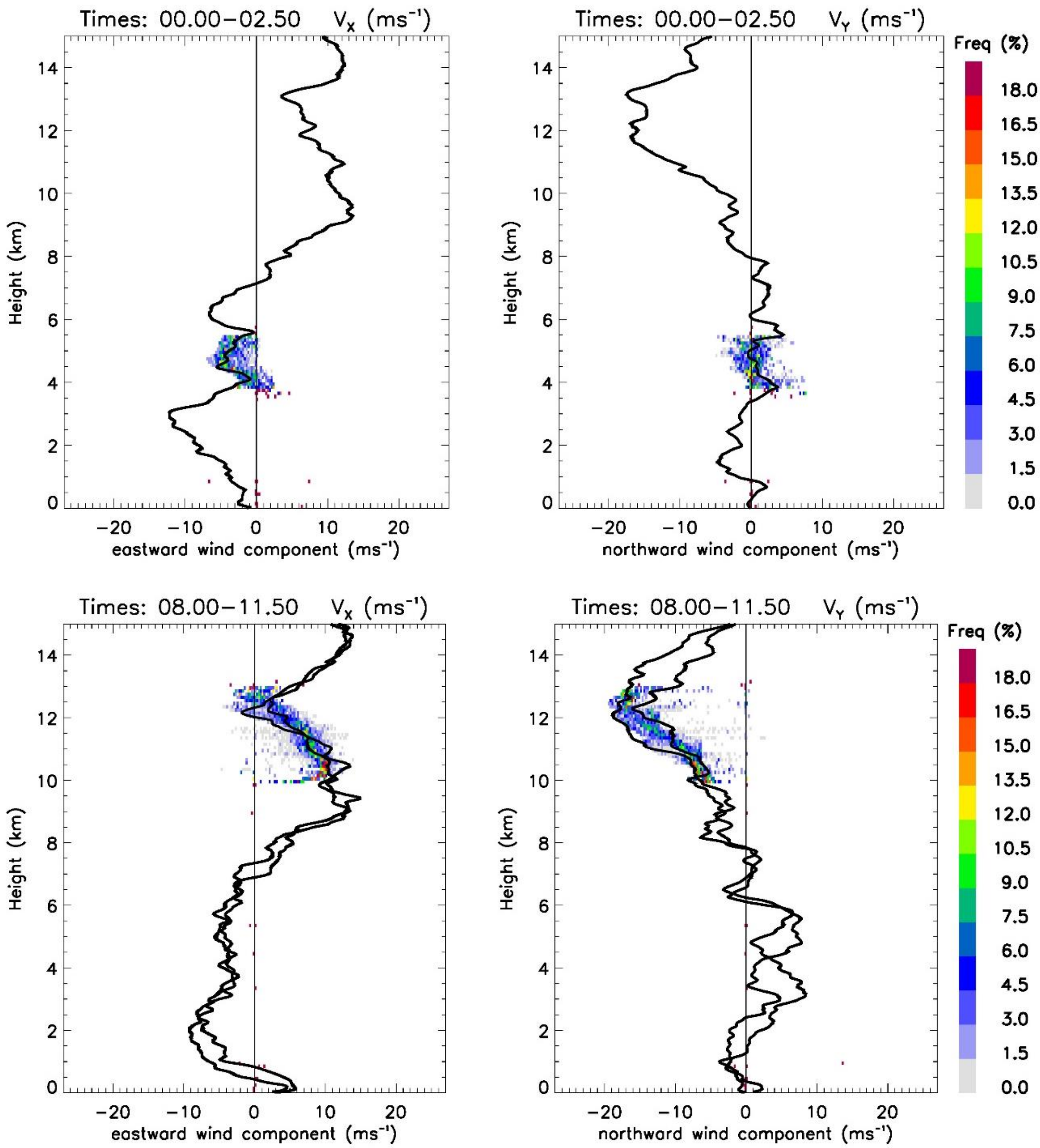

Figure 7: Same as Fig. 3 but for the altostratus (top panels) and tropical cirrus (bottom panels) cases sampled on 04/12/2019